Ghalei et al., http://www.jcb.org/cgi/content/full/jcb.201409056/DC1

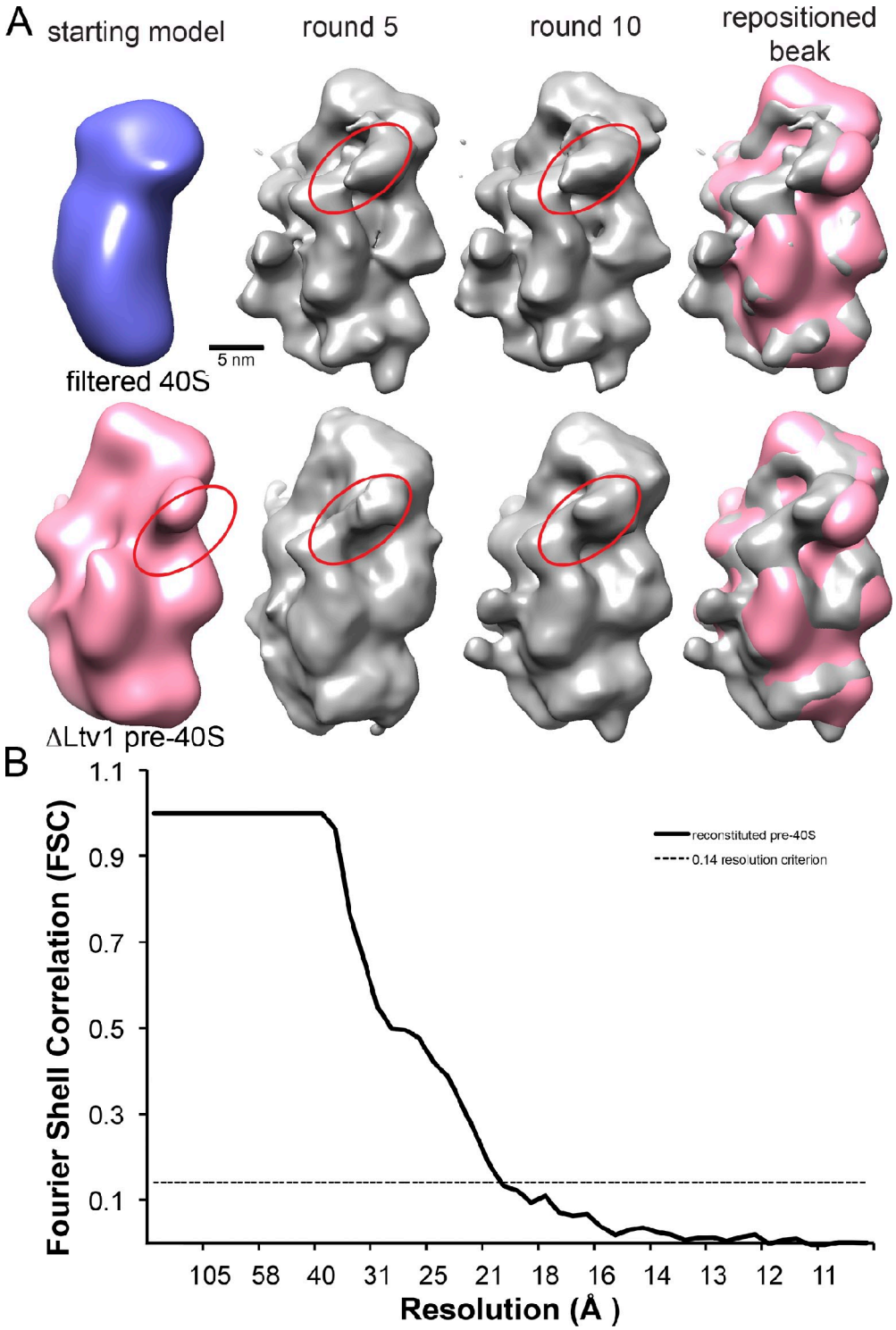

Figure S1. **Reconstitution of pre-40S ribosomes in vitro.** (A) Refinement of the reconstituted pre-40S against two different model results in structures that recapitulate native pre-40S. First, a heavily filtered model of the mature 40S subunit build from the x-ray crystal structure (Ben-Shem et al., 2011) was used as a starting model for projection matching refinement in EMAN (Ludtke et al., 1999). After five rounds, the retracted beak is resolved, and after five more rounds, the density of Ltv1 is apparent. Second, a heavily filtered model of the ΔLtv1 structure (EMD1924; Strunk et al., 2011) was used as a starting model. As before, after five rounds of projection matching the beak repositions, and after five more rounds of refinement the Ltv1 density is clear. Both resulting structures are superimposed on the ΔLtv1 structure to highlight the position of the retracted beak. The red circles highlight the beak and position of Ltv1. (B) The FSC curve calculated from two independently refined half-sets of data after convergence in Relion shows that the final model refines to a resolution of 21 Å.

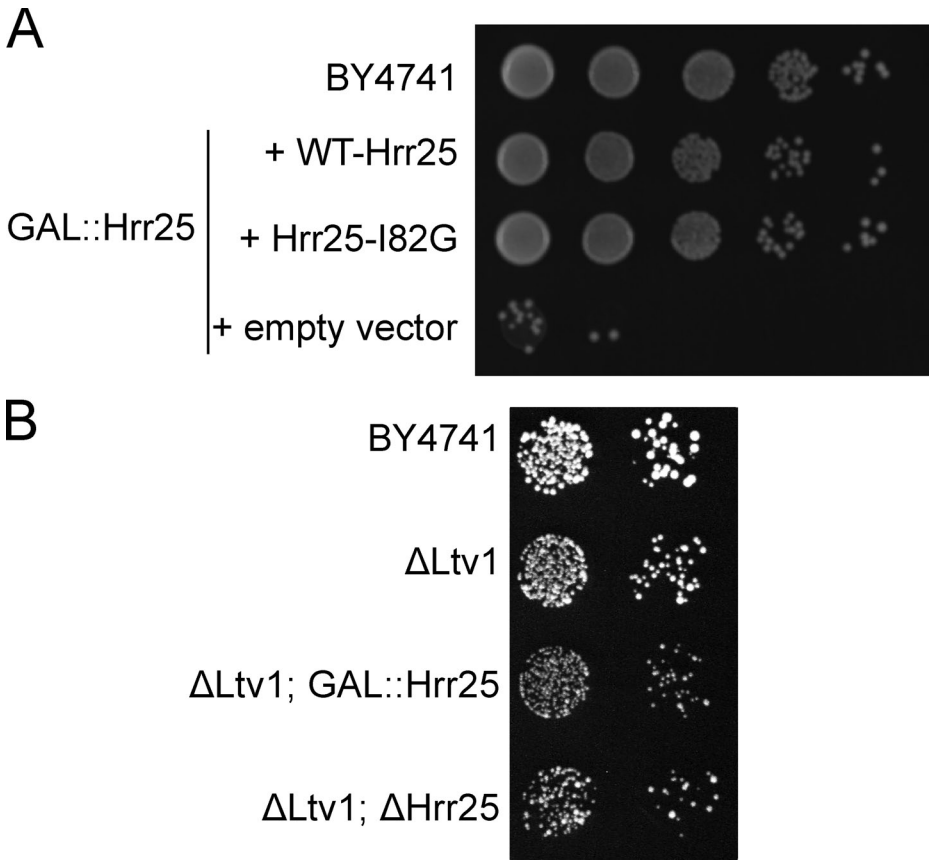

Figure S2. **The Hrr25-I82G mutant is fully functional in the absence of 1NA-PP1.** (A) Growth of wild-type yeast cells (BY4741) and cells containing galactose-inducible/glucose-repressible Hrr25 (GAL::Hrr25) carrying plasmids of wild-type (GAL::Hrr25+WT-Hrr25), ATP analogue-sensitive (GAL::Hrr25+Hrr25-I82G), or empty plasmid (GAL::Hrr25+empty vector), is compared on glucose-containing (YPGLU) plates at 30°C. (B) Close-up of Fig. 4 A to show the differences in colony size.

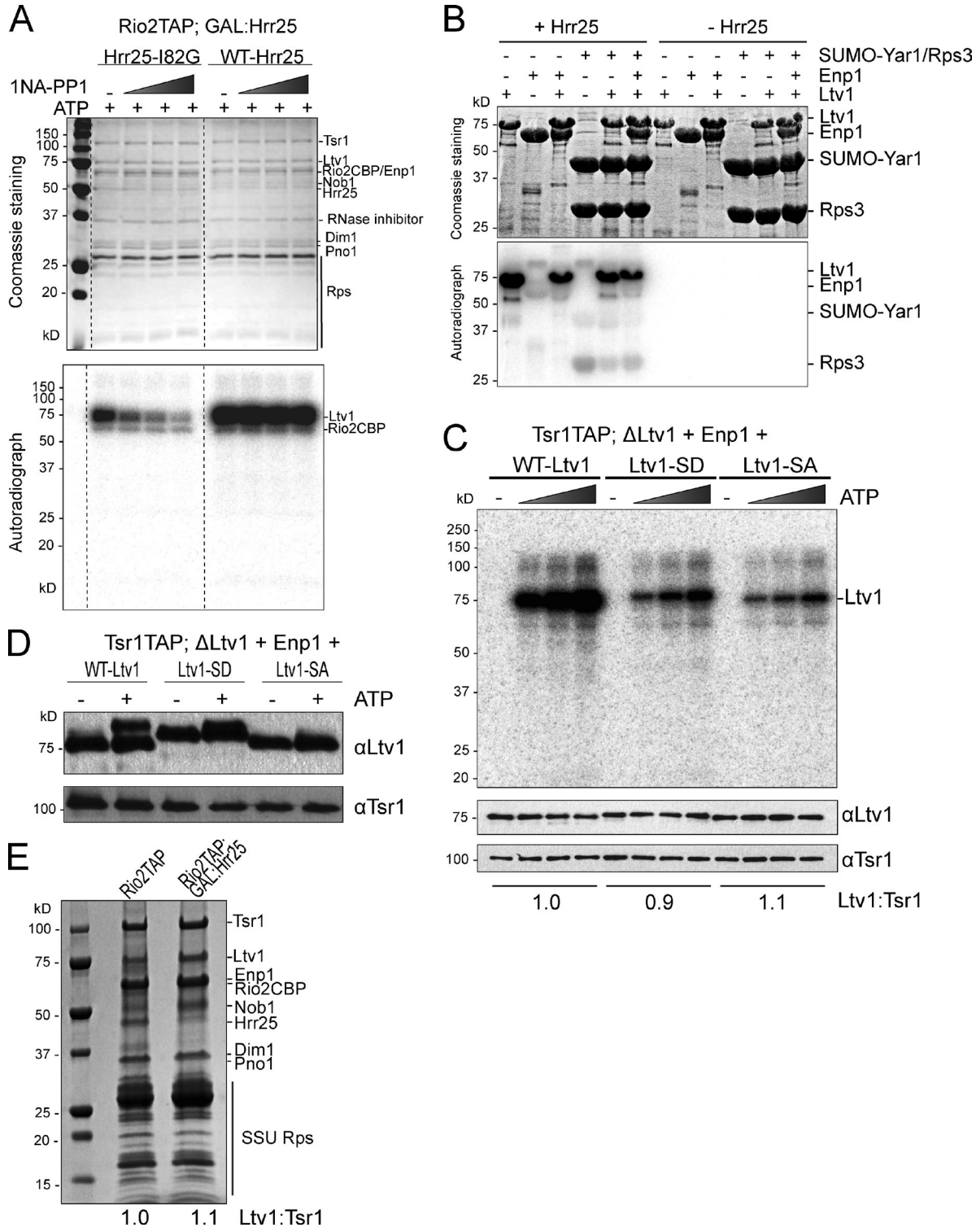

Figure S3. **In vitro phosphorylation of Ltv1 by Hrr25.** (A) Rio2TAP pre-40S ribosomes containing wild-type (WT-Hrr25) or 1-NA-PP1–sensitive Hrr25 (Hrr25-I82G) were assayed for in vitro phosphorylation using γ-[^{32}P]ATP and increasing concentrations of 1NA-PP. Reactions were analyzed on SDS-PAGE and stained with Coomassie blue. Phosphorylated proteins were detected by autoradiography of the dried gel. The broken lines indicate that intervening lanes were spliced out for presentation purposes. (B) Ltv1 and Ltv1/Enp1 are significantly phosphorylated, whereas Hrr25, Enp1, and Rps3 are only slightly phosphorylated. Recombinant Ltv1, Enp1, Yar1, and Rps3 were tested in an in vitro phosphorylation assay using γ-[^{32}P]ATP in the presence or absence of Hrr25. Reactions were analyzed on SDS-PAGE and stained with Coomassie blue. Phosphorylated proteins were detected by autoradiography of the dried stained gel. (C) Reduced phosphorylation of Ltv1-S/A and Ltv1-S/D. Pre-40S ribosomes from Tsr1-TAP;ΔLtv1 strains supplemented with plasmids encoding wild-type Ltv1, Ltv1-S/D, or Ltv1-S/A were purified. Increasing amounts of γ-[^{32}P]ATP were added before SDS-PAGE analysis. On the bottom are Western blot analyses of Tsr1 levels showing equal loading. The quantitation is for copurifying amounts of Ltv1. (D) Addition of 500 nM ATP to pre-40S purified as in C produces a band of lower electrophoretic mobility for wild-type Ltv1, but not Ltv1-S/A. Ltv1-S/D runs slower without the addition of ATP. ATP concentrations in this experiment are 20-fold higher than in the experiment shown in C. (E) SDS-PAGE of pre-40S ribosomes from cells lacking and containing Hrr25. Pre-40S ribosomes from cells lacking Hrr25 have 1.1-fold more Ltv1. Ltv1 occupancy in wild-type cells is >70%, providing an upper limit of a possible 1.3-fold increase.

Figure S4. **Sequence alignment of residues 322–386 of yeast Ltv1 and its homologues.** Species are identified on the left of the aligned sequences. A darker background indicates higher conservation. Conserved serine and threonine residues are highlighted in red. Blue arrowheads indicate the phosphosites that were identified and characterized in this study.

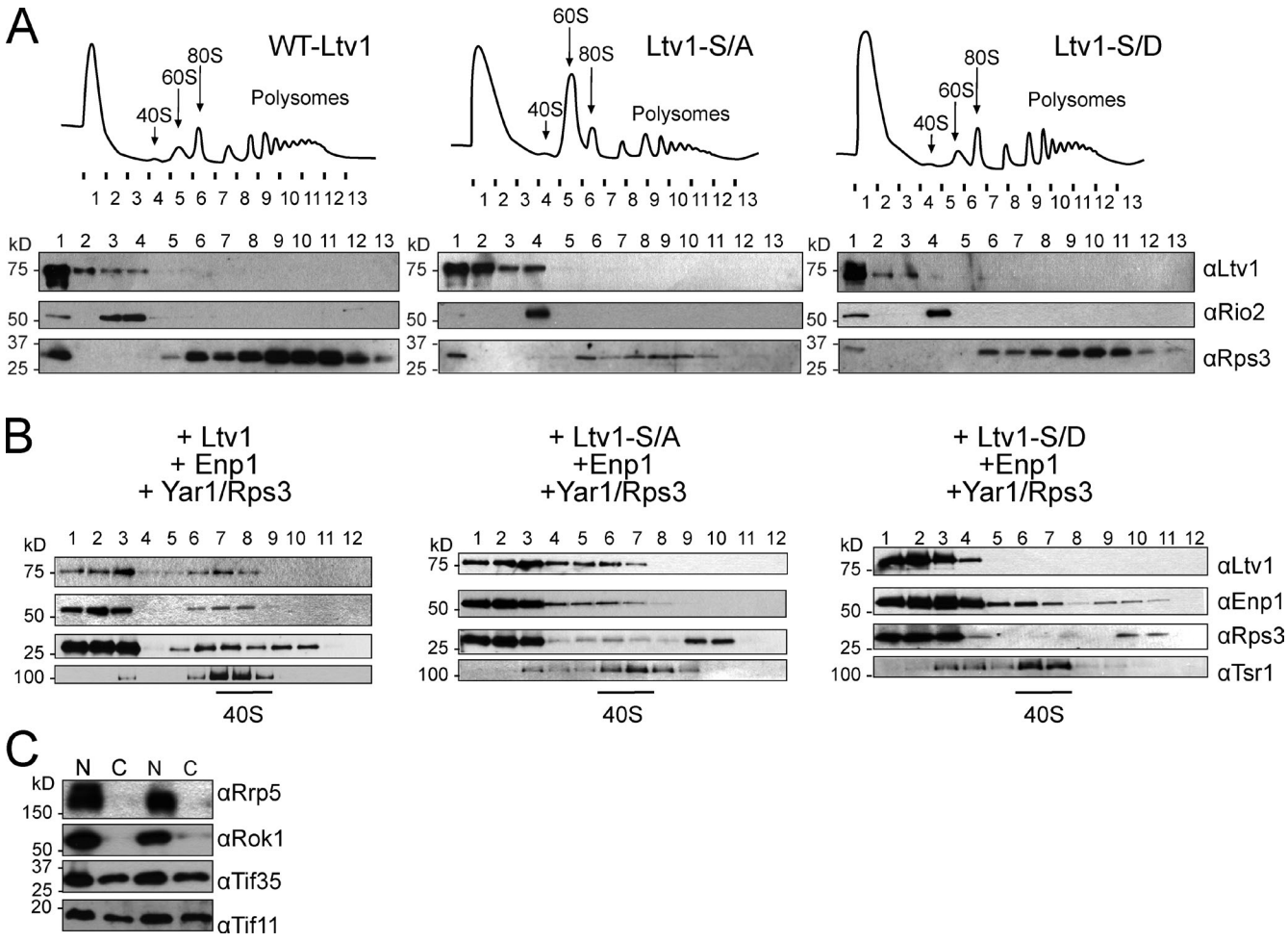

Figure S5. **Binding of Ltv1-S/A and Ltv1-S/D mutants to pre-40S ribosomes.** (A) 10–50% sucrose gradients of lysates from ΔLtv1 cells transformed with WT-Ltv1, Ltv1-S/D, or Ltv1-S/A plasmids. The top panels show the absorbance profiles at 254 nm and the bottom panels show Western blot analyses with the indicated antibodies. (B) 5–20% sucrose gradients from purified Rio2TAP pre-40S reconstituted with the indicated proteins, and analyzed by Western blotting. The position of 40S ribosomes is indicated. (C) Western blots of nuclear (N) and cytoplasmic (C) fractions after separation demonstrate that the cytoplasm is not significantly contaminated with nuclear proteins such as Rrp5 and Rok1.

Table S1. **Yeast strains used in this study**

Strain	Description	Genotype	Reference
YKK73	ΔLtv1	BY4741;Ltv1::KAN	Strunk et al., 2011
YKK352	Rio2TAP;ΔLtv1	BY4741;Rio2TAP::His; Ltv1::KAN	Strunk et al., 2011
YKK468	Tsr1TAP;ΔLtv1	BY4741;Tsr1TAP::His; Ltv1::KAN	This paper
YKK438	GAL1::Hrr25	BY4741;GAL1Hrr25::NAT	This paper
YKK439	ΔLtv1;GAL1::Hrr25	BY4741;Ltv1::KAN; GAL1Hrr25::NAT	This paper
YKK422	ΔLtv1;GAL1::Fap7	BY4741;Ltv1::KAN; GAL1Fap7::NAT	This paper
YKK284	GAL1::Hrr25; GAL1::Fap7	BY4741;GAL1Hrr25::NAT;GAL1Fap7::KAN	This paper
YKK560	ΔLtv1;ΔHrr25	BY4741;Ltv1::KAN;Hrr25::HYG	This paper

All deletions are complete deletions of the coding sequence using the indicated markers.

Table S2. **Plasmids used in this study**

Plasmid name	Description	Origin	Promoter	Reference
pKK193	pSV272-Ltv1[a]	Single copy	T7	Campbell and Karbstein, 2011
pKK199	pSV272-Enp1[a]	Single copy	T7	Campbell and Karbstein, 2011
pKK196	pGEX4T-3 (GE Healthcare)-Hrr25	Single copy	tac	Kafadar et al., 2003
pKK1230	pET28a SUMO-Rps3[b]	Single copy	T7	This paper
pKK1270	pET23 (EMD Millipore)-Enp1	Single copy	T7	This paper
pKK1285	pET28a-SUMO-Yar1[b]	Single copy	T7	This paper
pKK1288	pET-Duet1-Rps3	Single copy	T7	This paper
pKK1338	pSV272-Ltv1-S336/339/342A (Ltv1-S/A)	Single copy	T7	This paper
pKK1340	pSV272-Ltv1-S336/339/342D (Ltv1-S/D)	Single copy	T7	This paper
pKK3479	pRS416-TEF (ATCC 87368)-Hrr25	Single copy	TEF	This paper
pKK3478	pRS416-TEF-Hrr25-I82G	Single copy	TEF	This paper
pKK3345	pRS416-TEF-Ltv1	Single copy	TEF	This paper
pKK3554	pRS416-TEF-Ltv1-S/A	Single copy	TEF	This paper
pKK3557	pRS416-TEF-Ltv1-S/D	Single copy	TEF	This paper
pKK3647	pRS426-Gal1 (ATCC 77452)-Ltv1	Multi copy	Gal1	This paper
pKK3648	pRS426-Gal1-Ltv1-S/A	Multi copy	Gal1	This paper
pKK3649	pRS426-Gal1-Ltv1-S/D	Multi copy	Gal1	This paper
pKK500	pRETROX-dsREDmirE(Renilla)-GFP[c]		TRE3G	This paper
pKK501	pRETROX-dsREDmirE(hLtv1)-GFP[c]		TRE3G	This paper
pKK502	pRETROX-TIGHT_GFP-Tomato[c]		TRE3G	This paper
pKK503	pRETROX-TIGHT_GFP-hLtv1[c]		TRE3G	This paper
pKK504	pRETROX-TIGHT_GFP-hLtv1-S238/T241/S244A (hLtv1-S/A)[c]		TRE3G	This paper
pKK505	pRETROX-TIGHT_GFP-hLtv1- S238/T241/S244D (hLtv1-S/D)[c]		TRE3G	This paper
RIEP	MSCV-rtTA-IRES-Eco-Receptor-pgk-puro[d]		MSCV	Huang et al., 2014

[a]pSV272 is based on pET28a (EMD Millipore) and contains an N-terminal tag to produce His_6-MBP-TEV fusion proteins. MBP, maltose binding protein; TEV, tobacco etch protease.
[b]pET28SUMO is based on pET28a (EMD Millipore) and contains an N-terminal tag to produce His_6-SUMO fusion proteins.
[c]RetroX vectors are based on pRETROX-TRE3G from Takara Bio Inc.
[d]The RIEP vector (MSCV-rtTA-IRES-Eco-Receptor-pgk-puro) is based on MSCV-IRES-puro from Addgene.

References

Ben-Shem, A., N. Garreau de Loubresse, S. Melnikov, L. Jenner, G. Yusupova, and M. Yusupov. 2011. The structure of the eukaryotic ribosome at 3.0 Å resolution. *Science*. 334:1524–1529. http://dx.doi.org/10.1126/science.1212642

Campbell, M.G., and K. Karbstein. 2011. Protein-protein interactions within late pre-40S ribosomes. *PLoS ONE*. 6:e16194. http://dx.doi.org/10.1371/journal.pone.0016194

Huang, C.H., A. Lujambio, J. Zuber, D.F. Tschaharganeh, M.G. Doran, M.J. Evans, T. Kitzing, N. Zhu, E. de Stanchina, C.L. Sawyers, et al. 2014. CDK9-mediated transcription elongation is required for MYC addiction in hepatocellular carcinoma. *Genes Dev.* 28:1800–1814. http://dx.doi.org/10.1101/gad.244368.114

Kafadar, K.A., H. Zhu, M. Snyder, and M.S. Cyert. 2003. Negative regulation of calcineurin signaling by Hrr25p, a yeast homolog of casein kinase I. *Genes Dev.* 17:2698–2708. http://dx.doi.org/10.1101/gad.1140603

Ludtke, S.J., P.R. Baldwin, and W. Chiu. 1999. EMAN: semiautomated software for high-resolution single-particle reconstructions. *J. Struct. Biol.* 128:82–97. http://dx.doi.org/10.1006/jsbi.1999.4174

Strunk, B.S., C.R. Loucks, M. Su, H. Vashisth, S. Cheng, J. Schilling, C.L. Brooks III, K. Karbstein, and G. Skiniotis. 2011. Ribosome assembly factors prevent premature translation initiation by 40S assembly intermediates. *Science*. 333:1449–1453. http://dx.doi.org/10.1126/science.1208245